Mapping Arctic Slumps on Banks Island, NWT, Canada

Environment and Climate Change Canada – Algonquin College

Environment and Climate Change Canada

He Kang

ALGONQUIN COLLEGE

Introduction

Climate change has caused permafrost degradation and increased slump activities in the Canadian Arctic. These changes have negative effects on local communities, ecosystems, and Arctic landscape. Retrogressive thaw slumps are common landslides caused by melting of ground ice in permafrost. Dr. Zhaohua Chen from Environment and Climate Change Canada is leading a research project collaborated with Parks Canada to study coastal erosion and landscape changes in the Arctic. This project serves as a pilot project of Dr. Chen's research to study an area of about 513 km^2 within the Aulavik National Park on northern Banks Island, Northwest Territories.

This project systematically studied potential factors that could affect the occurrence of slump activities on Banks Island. The significance of topography, geology, land cover, and hydrology on Arctic slump activities was investigated using geographic information systems (GIS) methods. The final output of this project included three main deliverables: 1) a geodatabase with raster and vector datasets containing layers that influence slump activities; 2) regression analysis methods analyzing factors influencing slump activities; and 3) slump susceptibility maps of the study area.

Methods

Flow diagram of methodology is illustrated in Figure 1. A geodatabase was built in ArcGIS Pro to store slump inventory and all factor layers that could influence slump occurrence including topography, geology, land cover/use, and hydrology. Some derived layers included elevation, slope, aspect, bedrock geology, geological structures, bedrock dip angle and dip direction, dip direction and aspect difference, dip angle and slope difference, distance to structures, distance to flow, surficial geology, and land cover classification. Thematic maps were created for each factor layer. Values of all the factor layers at each slump occurrence were extracted using a model created in ArcGIS Model Builder and formed a slump inventory.

Before conducting regression analysis, continuous raster layers were normalized to value between 0 and 1, and categorical factor layers were broken down into binary raster layers. 500 random points outside of slump polygons were created and merged with the 88 slump origin points. Values of the modified raster layers were extracted to the 588 observation points. Linear and binary (logistic) regression analyses were conducted using IBM SPSS Statistics. Coefficients of variables and intercepts were used for calculating slump susceptibility at each pixel location within the study area.

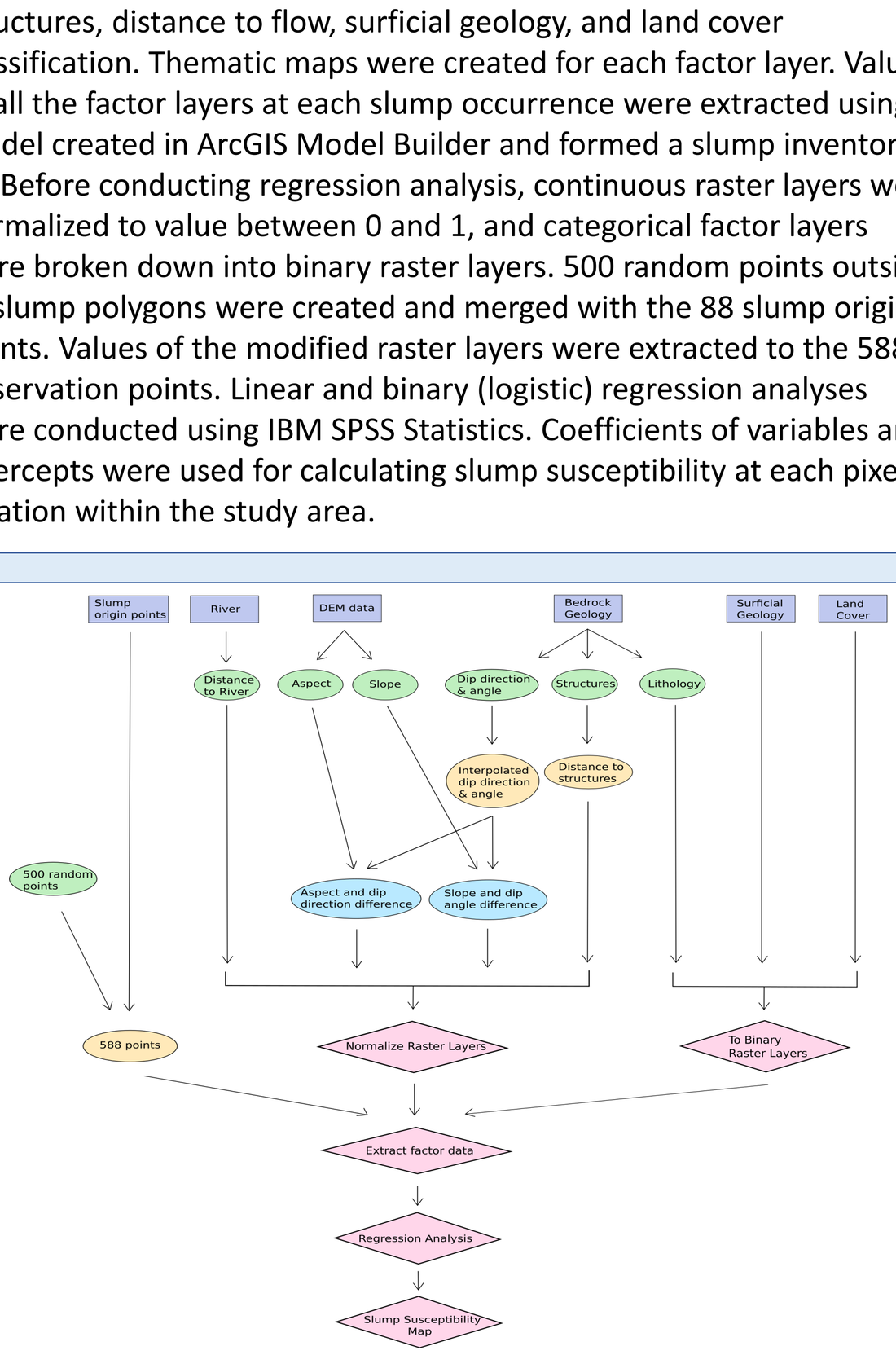

Figure 1. Flow diagram of methodology

Results

13 variables were chosen by IBM SPSS Statistics for a best-fitting linear regression result. The adjusted R square was 0.34. Binary regression result used 25 variables, and this model predicted 59.1% of the slump origin points and 97.2% of the non-slump points correctly (Table 1).

Figure 2 illustrates calculated raster layers based on regression analyses results. There was a significant difference between the slump susceptibility maps using two regression models. Results from the linear method indicated that most (75%) of the study area had slump probability between 0.2 and 0.4, whereas results from the binary method indicated that most (88%) of the study area had slump probability between 0 and 0.2. The binary method predicted more study area belonging to the medium high and high classes, which was 2.18% compared to 0.23% from the linear method. Despite these differences, areas of slump probability higher than 0.4 were relatively consistent in two slump susceptibility maps.

Variables	Unstandardized coefficients		Standardized coefficients	t (t-value)	Sig (p-value)
	Coefficients	Std. Error	Coefficients		
Constant	-0.03	0.07		-0.41	0.68
Slope	1.21	0.16	0.26	7.34	<0.001
Dip angle	0.39	0.10	0.15	3.88	<0.001
Dip direction	-0.39	0.06	-0.27	-6.85	<0.001
Anaclinal slope	0.13	0.03	0.15	4.37	<0.001
Distance to flow	-0.18	0.08	-0.08	-2.27	0.02
Geology – shale	0.11	0.04	0.12	2.56	0.01
Geology – mixed sedimentary rock	-0.15	0.06	-0.13	-2.65	0.01
Surficial geology – undifferentiated deposits	0.16	0.08	0.07	2.06	0.04
Surficial geology – till plain	-0.15	0.03	-0.21	-5.65	<0.001
Landcover – dryas snowbank	0.17	0.04	0.16	4.37	<0.001
Landcover – hydric subhydric fen	0.08	0.03	0.11	2.87	0.004
Landcover – water shadow	0.29	0.05	0.22	5.99	<0.001
Regression Statistics					
R	0.59				
R Square	0.35				
Adjusted R Square	**0.34**				
Std. Error of the Estimate	0.29				

Variables	Coefficients	Std. Error	Wald	df	Sig.	Exp(B)
Constant	5.50	23.71	0.05	1	0.82	246
Elevation	1.32	1.34	0.97	1	0.32	3.76
Aspect	-0.09	0.86	0.01	1	0.92	0.92
Slope	4.84	25.81	0.04	1	0.85	127
Dip angle	5.41	4.42	1.50	1	0.22	223
Dip direction	-3.89	1.02	14.54	1	<0.001	0.02
Cataclinal slope	-1.04	0.63	2.69	1	0.10	0.36
Orthoclinal slope	-1.07	0.42	6.59	1	0.01	0.34
Dip angle – slope difference	-5.06	27.73	0.03	1	0.86	0.01
Distance to flow	-2.53	1.42	3.15	1	0.08	0.08
Distance to geological structures	-1.73	1.04	2.74	1	0.1	0.18
Geology – mixed sedimentary rock	-19.27	4496	0	1	1	0
Geology – sand	-2.29	1.17	3.82	1	0.05	0.10
Surficial geology – alluvial	-18.74	6547	0	1	1	0
Surficial geology – bedrock raster	-0.57	0.78	0.54	1	0.47	0.57
Surficial geology – eolian	-15.78	11511	0	1	1	0
Surficial geology – glaciofluvial	-17.78	5397	0	1	1	0
Surficial geology – till plain	-2.08	0.76	7.52	1	0.01	0.12
Landcover – dryas snowbank	-1.13	0.68	2.75	1	0.01	0.32
Landcover – hydric subhydric fen	-1.88	0.60	9.68	1	0.002	0.15
Landcover – meadow fen	-21.20	6460	0	1	1	0
Landcover – mesic sedge herb	-2.97	0.78	14.70	1	<0.001	0.05
Landcover – sparsely vegetated sand	-1.25	1.37	0.84	1	0.36	0.29
Landcover – sedge fen	-4.08	1.24	10.87	1	<0.001	0.02
Landcover – submesic dryas	-2.25	0.71	9.89	1	0.002	0.11
Landcover – subxeric dryas	-3.63	1.35	7.18	1	0.01	0.03
Model Summary						
-2 Log likelihood	Cox & Snell R Square		Nagelkerke R Square			
259.57	0.33		0.58			
Classification Table (cut value is 0.5)						
	Observed	Predicted		Percentage correct		
		0	1			
Slump occurrence	0	486	14	97.2		
	1	36	52	59.1		
Overall percentage				91.5		

Table 1. Regression analyses results (left: linear model, right: binary model)

$$P = \frac{e^{(\beta_0 + \beta_1 X_1 + \beta_2 X_2 + \ldots + \beta_k X_k)}}{1 + e^{(\beta_0 + \beta_1 X_1 + \beta_2 X_2 + \ldots + \beta_k X_k)}} \qquad P = \beta_0 + \beta_1 X_1 + \beta_2 X_2 + \ldots + \beta_k X_k$$

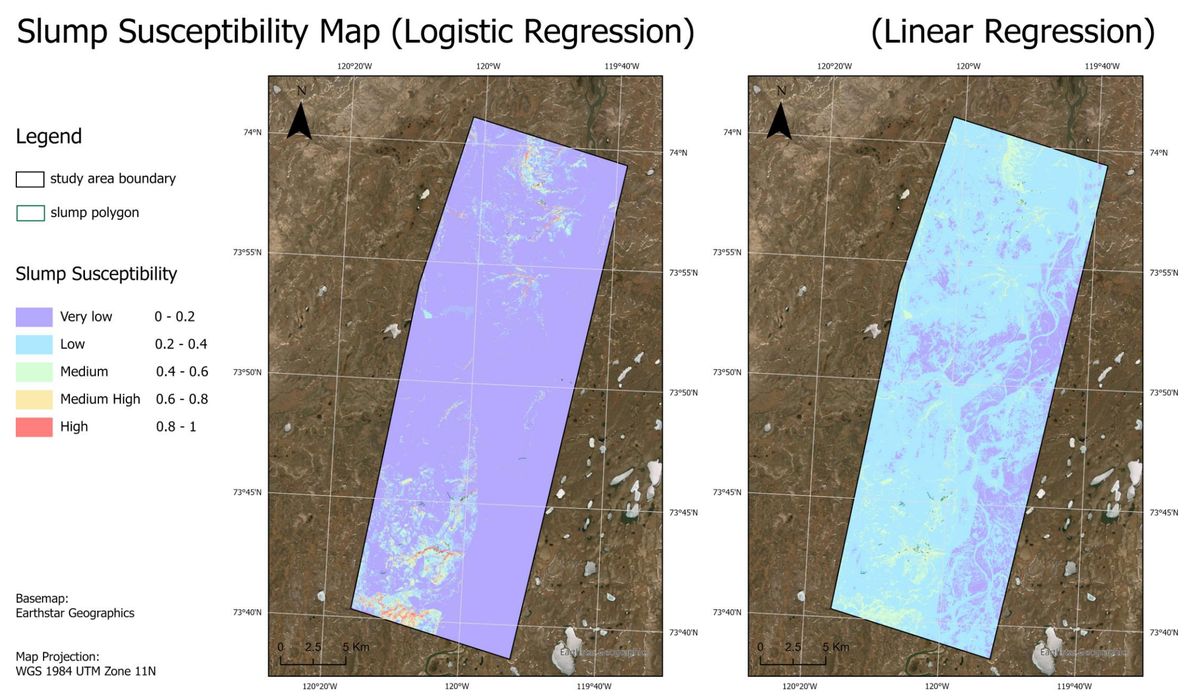

Figure 2. Slump Susceptibility Map

Conclusions

Linear and logistic regression models were built to map Arctic slumps on northern Banks Island, and two slump susceptibility maps were created. The study area was classified into five classes of slump susceptibility. The areas of medium to high slump susceptibility coincided well with observed slump occurrences.

Special thanks to Dr. Zhaohua Chen from Environment and Climate Change Canada for sponsoring this project and providing guidance on conducting data analysis. Thanks to Mike Ballard of Algonquin College for project management supervision.